

Analysis of the Palierne model by relaxation time spectrum

Mi Kyung Kwon^{1,2} and Kwang Soo Cho^{1,*}

¹*Department of Polymer Science and Engineering, School of Applied Chemical Engineering,
Kyungpook National University, Daegu 41566, Republic of Korea*

²*Division of Nano and Energy Convergence Research, Daegu Gyeongbuk Institute of Science and Technology (DGIST),
Daegu 42988, Republic of Korea*

(Received February 24, 2015; final revision received December 6, 2015; accepted December 15, 2015)

Viscoelasticity of immiscible polymer blends is affected by relaxation of the interface. Several attempts have been made for linear viscoelasticity of immiscible polymer blends. The Palierne model (1990) and the Gramespacher-Meissner model (1992) are representative. The Gramespacher-Meissner model consists of two parts: ingredients and interface. Moreover, it provides us the formula of the peak of interface in weighted relaxation time spectrum, which enables us to analyze the characteristics relating to interface more obviously. However, the Gramespacher-Meissner model is a kind of empirical model. Contrary to the Gramespacher-Meissner model, the Palierne model was derived in a rigorous manner. In this study, we investigated the Palierne model through the picture of the Gramespacher-Meissner model. We calculated moduli of immiscible blend using two models and obtained the weighted relaxation time spectra of them. The fixed-point iteration of Cho and Park (2013) was used in order to determine the weighted relaxation spectra.

Keywords: immiscible polymer blend, the Palierne model, the Gramespacher-Meissner model, relaxation time spectrum, fixed-point iteration method

1. Introduction

Several theories have been developed to describe rheological properties of immiscible blends. Choi and Schowalter (1975) developed a rheological model for immiscible mixture of two Newtonian fluids. The model assumes that dispersed phase has a finite size as emulsion particle. This assumption is reasonable for mixtures with low concentration of dispersed phase, while it is difficult to recognize dispersed phase when concentrations of two components are comparative. When co-continuous structure appears, there is no characteristic length scale. Doi and Ohta (1991) developed a rheological model which can describe such co-continuous binary mixtures of Newtonian fluids. Thus the approach of the Doi and Ohta theory is totally different from that of the Choi and Schowalter. The Gramespacher and Meissner model (1992) was developed by modification of the Choi and Schowalter model in order to describe linear viscoelasticity of immiscible polymer blends which have characteristic size of dispersed phase. Lee and Park (1994) extended the Doi and Ohta model to the immiscible polymer blends. Compared with these models, the Palierne model (Palierne, 1990) is considered as the most rigorous one for blends of polymers. In linear viscoelastic regime, the Palierne model was derived for blends of

the incompressible viscoelastic materials. Additionally, it includes previous results for various types of mixtures such as the mixture of two Newtonian fluids, the mixture of elastic solid in Newtonian fluid, the mixture of elastic solid in viscoelastic fluid, and so on (Shonaike and Simon, 1999).

There have been a number of studies applying the above models to various immiscible blends. While the Lee-Park model consists of differential equations which are hard to be solved analytically, it is more convenient to use the Palierne model or the Gramespacher-Meissner model (GM model) which are expressed in algebraic equation. The Palierne model was derived from rigorous theoretical foundation, while the GM model is an empirical model modified from the model of Choi and Schowalter. However, the GM model provides physical insights on interfacial relaxation contrary to the Palierne model due to the separability of formula. One of the most important features of the GM model is to provide a new insight that relaxation time spectrum of immiscible mixture can be decomposed to the contributions from ingredients and interface. This cannot be recognized from the Palierne model because its equation cannot be decomposed into two parts. In here, the Palierne model will be analyzed by the learning from the GM model.

After shear deformation, the dispersed phase of immiscible blend is recovered into spherical shape on account of the interfacial tension between the components. The relaxation behavior of interfaces gives rise to additional visco-

[#]This article was presented at the 6th Pacific Rim Conference on Rheology (PRCR), held on 20-25 July, 2014, Australia.

*Corresponding author; E-mail: polphy@knu.ac.kr

elastic effect to the blend. As the content of dispersed phase increases, the relaxation of interface reduces the slope of storage modulus in the terminal region while no significant changes are observed in loss modulus in the terminal region. Although variation of storage modulus due to structures of immiscible blend is found in both models and experiments, the variation is not large enough to quantitatively detect the difference in the structure. However, it was found that the weighted relaxation spectrum was very sensitive to the structural changes of immiscible blends (Gramespacher and Meissner, 1992). Weighted relaxation spectrum is the product of relaxation time and relaxation spectrum. Although peak-like shapes are not easily recognized in relaxation time spectrum, weighted relaxation spectrum of immiscible blends allows us to identify peaks of ingredients and that of interface, which can be understood easily by the GM model (Gramespacher and Meissner, 1992). We call this feature of the GM model the picture of the GM model. Hence, the main purpose of this paper is to analyze the rigorous Palierne model in the picture of the GM model.

Since the relaxation spectrum is calculated from viscoelastic data and suffers from ill-posedness (Honerkamp, 1989), the use of weighted spectrum depends on how reliable algorithm is used. The method used here is the modified version of the fixed-point iteration method developed by Cho and Park (2013). In order to obtain spectra which reflect the property of immiscible blend well, we shall suggest and compare various modification of the fixed-point iteration.

2. Theoretical Background

2.1. The Palierne model

When we know the linear viscoelasticity of pure components, the composition, the interfacial tension and the size distribution of dispersed phase, the linear viscoelasticity of the blend can be predicted from the Palierne model as follows (Graebling *et al.*, 1993);

$$G_{\text{ble}}^*(\omega) = G_{\text{mat}}^*(\omega) \frac{1 + 3 \sum_i \varphi_i P_i^*(\omega)}{1 - 2 \sum_i \varphi_i P_i^*(\omega)}, \quad (1)$$

$$P_i^*(\omega) = \frac{\left[\begin{array}{l} 4 \frac{\alpha}{R_i} \{2G_{\text{mat}}^*(\omega) + 5G_{\text{dis}}^*(\omega)\} \\ - \{G_{\text{mat}}^*(\omega) - G_{\text{dis}}^*(\omega)\} \cdot \{16G_{\text{mat}}^*(\omega) + 19G_{\text{dis}}^*(\omega)\} \end{array} \right]}{\left[\begin{array}{l} 40 \frac{\alpha}{R_i} \{G_{\text{mat}}^*(\omega) + G_{\text{dis}}^*(\omega)\} \\ + \{3G_{\text{mat}}^*(\omega) + 2G_{\text{dis}}^*(\omega)\} \cdot \{16G_{\text{mat}}^*(\omega) + 19G_{\text{dis}}^*(\omega)\} \end{array} \right]} \quad (2)$$

where G_{mat}^* , G_{dis}^* and G_{ble}^* are the complex moduli of the matrix phase, the dispersed phase, and the blend, α is

the interfacial tension between two components, and φ_i is the volume fraction of the dispersed phase with the radius R_i . Besides, terms related with size distribution of dispersed phase are included. However, it is not easy to understand the effect of interface from taking a look at the equation.

2.2. The Gramespacher-Meissner model

The Gramespacher-Meissner model can be decomposed into two parts of pure components and interface clearly, which suggests us insightful point of view. Complex modulus of a blends are the sum of the arithmetic mean of moduli for components and that for interface as follows;

$$G_{\text{ble}}^*(\omega) = \varphi G_{\text{dis}}^*(\omega) + (1 - \varphi) G_{\text{mat}}^*(\omega) + G_{\text{int}}^*(\omega), \quad (3)$$

$$G'_{\text{int}}(\omega) = \frac{\eta}{\lambda_{\text{int}}} \left(1 - \frac{\lambda_2}{\lambda_{\text{int}}} \right) \frac{(\omega \lambda_{\text{int}})^2}{1 + (\omega \lambda_{\text{int}})^2}, \quad (4)$$

$$G''_{\text{int}}(\omega) = \frac{\eta}{\lambda_{\text{int}}} \left(1 - \frac{\lambda_2}{\lambda_{\text{int}}} \right) \frac{\omega \lambda_{\text{int}}}{1 + (\omega \lambda_{\text{int}})^2}, \quad (5)$$

$$\eta = \eta_{\text{mat}}^0 \left[1 + \varphi \frac{5k+2}{2(k+1)} + \varphi^2 \frac{5(5k+2)^2}{8(k+1)^2} \right], \quad (6)$$

$$\lambda_{\text{int}} = \lambda_0 \left[1 + \varphi \frac{5(19k+16)}{4(k+1)(2k+3)} \right], \quad (7)$$

$$\lambda_2 = \lambda_0 \left[1 + \varphi \frac{3(19k+16)}{4(k+1)(2k+3)} \right], \quad (8)$$

$$\lambda_0 = \frac{\eta_{\text{mat}}^0 R (19k+16)(2k+3)}{\alpha 40(k+1)}, \quad (9)$$

$$k = \frac{\eta_{\text{dis}}^0}{\eta_{\text{mat}}^0} \quad (10)$$

where G'_{int} and G''_{int} are the storage and loss moduli caused by interfaces, η_{mat}^0 and η_{dis}^0 are the zero shear viscosities of the matrix and the dispersed phase, respectively, and R is the average radius of the dispersed phase. This structure of equation implies that the weighted relaxation spectrum of blend consists of three main peaks: two for pure components and one for interface. From now on, let's call the additional peak the interface peak (Gramespacher and Meissner, 1992). Since the interface term of Eq. (3) is equivalent to the Maxwell model, the height of the interface peak can be interpreted as follows;

$$P_{\text{max}} \equiv \lambda_{\text{int}} H_{\text{int}} = \eta \left(1 - \frac{\lambda_2}{\lambda_{\text{int}}} \right). \quad (11)$$

2.3. Algorithms for relaxation time spectrum

If continuous spectrum $H(\lambda)$ is given, then dynamic

moduli can be calculated by

$$G'(\omega) = \int_{-\infty}^{\infty} K'(\lambda\omega)H(\lambda)d\log\lambda, \quad (12a)$$

$$G''(\omega) = \int_{-\infty}^{\infty} K''(\lambda\omega)H(\lambda)d\log\lambda \quad (12b)$$

where

$$K'(x) = \frac{x^2}{1+x^2}, \quad K''(x) = \frac{x}{1+x^2}. \quad (13)$$

Discrete spectrum can be considered as an approximation of continuous one because

$$G'(\omega) = \sum_{n=1}^{N_\lambda} K'(\lambda_n\omega)h_n, \quad G''(\omega) = \sum_{n=1}^{N_\lambda} K''(\lambda_n\omega)h_n. \quad (14)$$

Note that the mean-value theorem gives (Baumgaertel and Winter, 1992)

$$H(\lambda_n) = \frac{h_n}{\log(\lambda_{n+1}/\lambda_n)}. \quad (15)$$

If choosing N_λ relaxation times equally spaced in logarithmic scale, application of least square method to Eq. (14) might give a discrete relaxation time $\{\lambda_n\}$ and use of Eq. (15) converts it to the continuous spectrum. However, it was shown that a linear regression must not produce robust continuous spectrum (Honerkamp and Weese, 1989).

The fixed-point algorithm was developed to calculate continuous relaxation spectrum from loss modulus. The method is based on following iterative equation;

$$h_n^{(r+1)} = h_n^{(r)} \frac{\sum_{\alpha=1}^{N_\omega} K''_{n\alpha} G''_{\alpha}}{\sum_{k=1}^{N_\lambda} \left(\sum_{\beta=1}^{N_\omega} K''_{n\beta} K''_{k\beta} \right) h_k^{(r)}} \quad (16)$$

where G''_{α} is the loss modulus at the α^{th} frequency ω_{α} , $h_n^{(r)}$ is the relaxation intensity of r^{th} iteration at n^{th} relaxation time λ_n , N_ω is the number of frequency which is the number of data, N_λ is the number of relaxation times which will be chosen depending on how precisely spectrum will be calculated and the kernel matrix $K''_{n\alpha}$ is $K''(\lambda_n\omega_{\alpha})$.

The success of the fixed-point iteration relies mainly on the character of the kernel. If the kernel is replaced by that of storage modulus $K'_{n\alpha} = \lambda_n\omega_{\alpha}K''_{n\alpha}$ and loss modulus is replaced by storage modulus, then poor results are usually obtained. It is because the symmetric matrix in the denominator of Eq. (16) is not diagonal dominant when such replacement is done (Cho and Park, 2013). Eq. (16) implies that the resulting spectrum is always positive whenever the initially guessed spectrum is positive.

As mentioned earlier, loss modulus of immiscible blends is nearly independent of the content of dispersed phase.

Hence, the original fixed-point iteration must be modified. The modification can be done by remaining the kernel of loss modulus and changing data from loss modulus to storage modulus. Note that the variation of storage modulus is larger than that of loss modulus when structure of blends is changed.

The relation between storage modulus and relaxation spectrum is given as follows;

$$\eta''(\omega) = \frac{G'(\omega)}{\omega} = \int_{-\infty}^{\infty} K''(\lambda\omega)\lambda H(\lambda)d\log\lambda. \quad (17)$$

Eq. (17) is obtained by dividing ω on both sides of Eq. (12a). Then we can use $\eta''(\omega_{\alpha})$ as the data and the iteration equation is modified by

$$h_n^{(r+1)} = h_n^{(r)} \frac{\sum_{\alpha=1}^{N_\omega} K''_{n\alpha} \eta''_{\alpha}}{\sum_{k=1}^{N_\lambda} \left(\sum_{\beta=1}^{N_\omega} K''_{n\beta} K''_{k\beta} \right) \lambda_k h_k^{(r)}}. \quad (18)$$

Note that Eq. (18) is very similar to Eq. (16). Although Eq. (16) uses loss modulus as data while Eq. (18) uses storage modulus divided by frequency, the two equations share the same kernel matrix $K''_{n\alpha}$. For convenience, we call the original algorithm of Eq. (16) the G'' algorithm and the algorithm of Eq. (18) the η'' algorithm.

The iteration will be stopped when the following sum of square error shows the minimum;

$$\chi = \sqrt{\frac{1}{N} \sum_{\alpha=1}^{N_\omega} \left\{ \left[1 - \frac{G'_{\text{exp}}(\omega_{\alpha})}{G'_{\text{cal}}(\omega_{\alpha})} \right]^2 + \left[1 - \frac{G''_{\text{exp}}(\omega_{\alpha})}{G''_{\text{cal}}(\omega_{\alpha})} \right]^2 \right\}} \quad (19)$$

where the subscript ‘‘exp’’ indicates the modulus data while ‘‘cal’’ means the modulus calculated by Eq. (12) from the spectrum calculated by the iteration.

3. Experimental

3.1. Preparation of samples

We chose polypropylene (PP) provided by Korea Petrochemical Ind. Co., Ltd and polystyrene (PS) purchased from Sigma-Aldrich as components of blends. The specifications of those samples are listed in Table 1.

The components were mixed in a Brabender Plastimeter at rotor speed of 50 rpm at 200°C for 5 minutes. The neat PS and PP were experienced in the same thermal

Table 1. Specifications for components of the blend.

	M_w [g/mol]	M_n [g/mol]	MI [g, ASTM-D1238]
Polystyrene	350,000	170,000	-
Polypropylene	340,000	-	3.4

history. The resulting blends had weight fractions of 8, 10, 12, 14, and 16% PP in PS. In order to avoid the degradation of polymers, 0.15 phr of Irganox 1076 was added as an anti-oxidant. After mixing, the samples were pressed for making the shape of a disk under pressures at 200°C for 5 minutes.

3.2. Rheological measurements

The stress-controlled rheometer, AR2000ex was used in equipped with the parallel plate with the radius of 25 mm. Immiscible polymer blends often do not satisfy the principle of time-temperature superposition. Thus the dynamic tests were carried out in the range of frequency from 0.01 rad/s to 100 rad/s at 250°C under an atmosphere of nitrogen. Zero shear viscosities of PS and PP are 1010 and 2360 Pa·s.

4. Results and Discussion

4.1. Comparison of the models with experimental data

In order to test the validity of the GM and the Palierne models, volume fraction of dispersed phase is needed as well as the ratio of interface tension to the size of dispersed phase. The volume fraction of dispersed phase ϕ is described with the weight fraction, w as follows;

$$\phi = \frac{w}{w + r(1 - w)} \quad (20)$$

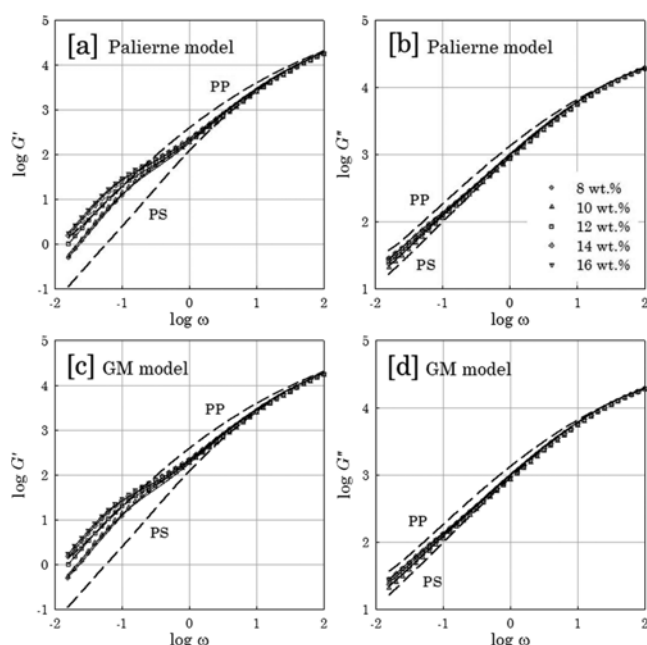


Fig. 1. Comparison between experimental data and results from fitting to two models, the Palierne model ((a) and (b)) and the GM model ((c) and (d)). (a) and (c) are storage moduli and loss moduli are shown in (b) and (d). Solid lines are fitting results. Symbols and dashed lines denote experimental data of blends and components, respectively.

where r is the ratio of densities of dispersed and matrix phases;

$$r = \frac{\rho_{\text{mat}}}{\rho_{\text{dis}}} \quad (21)$$

However, it is not easy to measure density of polymer melts at a given temperature. Furthermore, it is also difficult to measure precisely interfacial tension and the radius of dispersed phase. Hence, we used ϕ and α/R as the fitting parameter for the two models. Fig. 1 shows how well the two models fit experimental data when ϕ and α/R are considered as fitting parameters.

However, unfortunately, the volume fractions ϕ determined by the regression do not agree with Eq. (20). Furthermore, α/R was different for each weight fraction. From this result, we guess that the dispersed and matrix phases might not be pure PP and pure PS, respectively. The regression results for volume fraction was the same irrespective of models while α/R shows different values depending on models as shown in Table 2. Compared with the results of Gramspacher and Meissner (1992), our experimental data deviate a little bit more from the models. It can be explained that the density ratio r of PS and PMMA used by Gramspacher and Meissner is closer to unity while that of our material (PS and PP) is known much larger than unity.

One may say that it is one of the most efficient ways to show prediction of calculated moduli with parameters such as interfacial tension and radius and compare them to moduli measured experimentally in order to compare the two models. However, results of prediction through both models are affected by the accuracy of parameters such as interfacial tension, radius, and volume fraction. Since interfacial tension α is an equilibrium thermodynamic quantity, the measurement of α requires waiting time to equilibrium, which increases as molecular weight. Hence, most experimental data of interfacial tension in literature have been obtained from considerably low molecular weight samples. SEM or TEM may be a candidate for the measurement of R . However, 2D image is not exact in finding average R . Moreover, it cannot be believed that both disperse and matrix phases consist of their own pure ingredients. If PP is a minor ingredient of the PP/PS mixture, then the disperse phase must be PP-rich phase and the matrix one must be PS-rich phase. Even if we know

Table 2. Regression results obtained by two models.

Models	8 wt.%	10 wt.%	12 wt.%	14 wt.%	16 wt.%	
Palierne	ϕ [vol.%]	15	14	20	26	27
	α/R [Pa]	661	479	389	347	309
GM	ϕ [vol.%]	15	14	21	26	27
	α/R [Pa]	1072	708	646	575	501

Table 3. Comparison of χ values using three different algorithms.

Algorithm	pure PS	8 wt.%	10 wt.%	12 wt.%	14 wt.%	16 wt.%	pure PP
from G''	0.0032	1.8	0.24	0.89	0.36	0.53	1.1
from η''	0.0027	0.0023	0.0018	0.0029	0.0027	0.0030	0.0065

the density of each pure ingredient as a function of temperature, we cannot determine exact value of the volume fraction of the disperse phase. The difficulty of measuring the parameters could lead to poor prediction regardless of the type of model used. Therefore, we generate moduli of blend from the two models using arbitrary value of α/R and the measured moduli of pure PP and PS as components and compare the simulated moduli each other instead of fitting them to moduli measured experimentally.

4.2. Comparison of two algorithms of the fixed-point iteration method

In order to decide an algorithm appropriate to blend systems, we compared results using two algorithms. We could observe that variation in content of PP made little change in loss modulus while outstanding change of storage modulus was shown in frequency region lower than 1 rad/s (Fig. 1). Storage modulus becomes larger in terminal

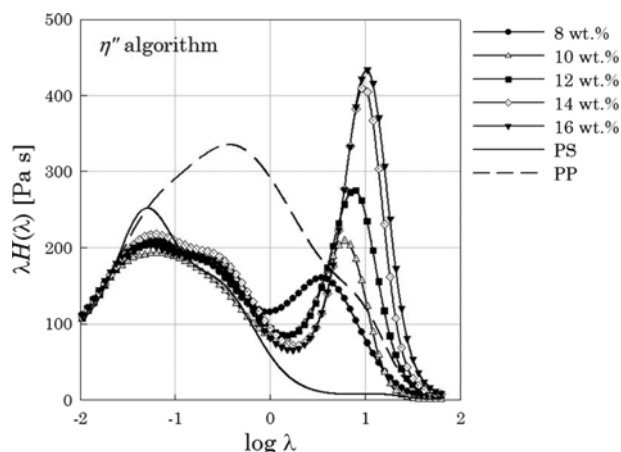


Fig. 2. Weighted relaxation time spectra calculated from the η'' algorithm of the fixed-point iteration. Lines represent weighted spectra of components and symbols with lines are those of blends with different contents of PP.

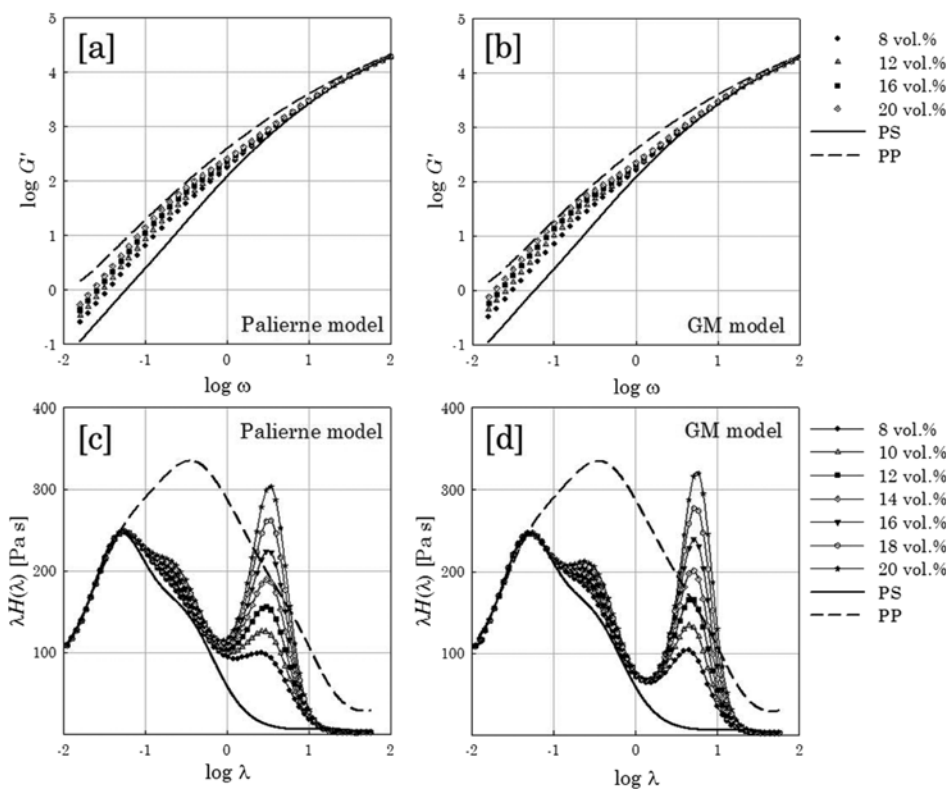


Fig. 3. Effect of the volume fraction of dispersed phase. Storage moduli generated from the Palierne model (a) and the GM model (b). Weighted relaxation time spectra are calculated from moduli using the Palierne model (c) and the GM model (d). Lines represent components and symbols or symbols with lines are blends with different contents of dispersed phase.

region as a content of dispersed phase rises. We tested two algorithms: the original algorithm using G'' , Eq. (16) and the algorithm using η'' , Eq. (18). The results are listed in Table 3. We evaluated χ values defined by Eq. (19). Eq. (18) resulted in better χ values than those from the original algorithm as expected earlier. From this result, we chose the algorithm using η'' throughout this study.

Fig. 2 shows weighted relaxation time spectra obtained by the modified algorithm of the fixed-point iteration. The weighted spectra of blends look like the sum of the average weight spectra of pure PP and PS and additional one. The additional peak becomes higher as content of dispersed phase increases. This peak is considered as the interfacial relaxation. The center of interfacial peak moves to longer relaxation time as content of dispersed phase increases.

4.3. Comparison of the Palierne model with the GM model

We generated dynamic moduli of various blends by the two models and the weighted relaxation time spectra were calculated from those in order to compare the two models quantitatively. Note that the symbols in Fig. 3 are simulated data calculated by the models and the lines are data of pure components. Blends are composed of dispersed

phase PP and matrix phase PS. All the blends are assumed that they have uniform dispersions with the radius of $1 \mu\text{m}$.

Fig. 3 shows the storage moduli and weighted spectra of various volume fractions of dispersed phase with a fixed $\alpha/R = 10^3 \text{ Pa}$. As the amount of PP increases, interface peak becomes higher and peak position shifts to longer time region in both models.

For a given volume fraction of dispersed phase, 12 vol.%, we investigated the effect of the ratio α/R as shown in Fig. 4. It is noteworthy that the ratio α/R has the dimension of stress. Hence, the ratio α/R can be considered as the characteristic stress of interface. We varied the ratio α/R in logarithm scale and m denotes exponent of the ratio in Fig. 4. As the characteristic stress of interface α/R increases, the position of interfacial peak moves to shorter relaxation time. From Figs. 3 and 4, we can make a conclusion that the two models shows almost the same behaviors although the two models have completely different formula.

The main feature of the GM model is the decomposition of the linear viscoelasticity to the contributions from pure components and interface. To check whether this feature is valid for the Palierne model, we subtract the contribution

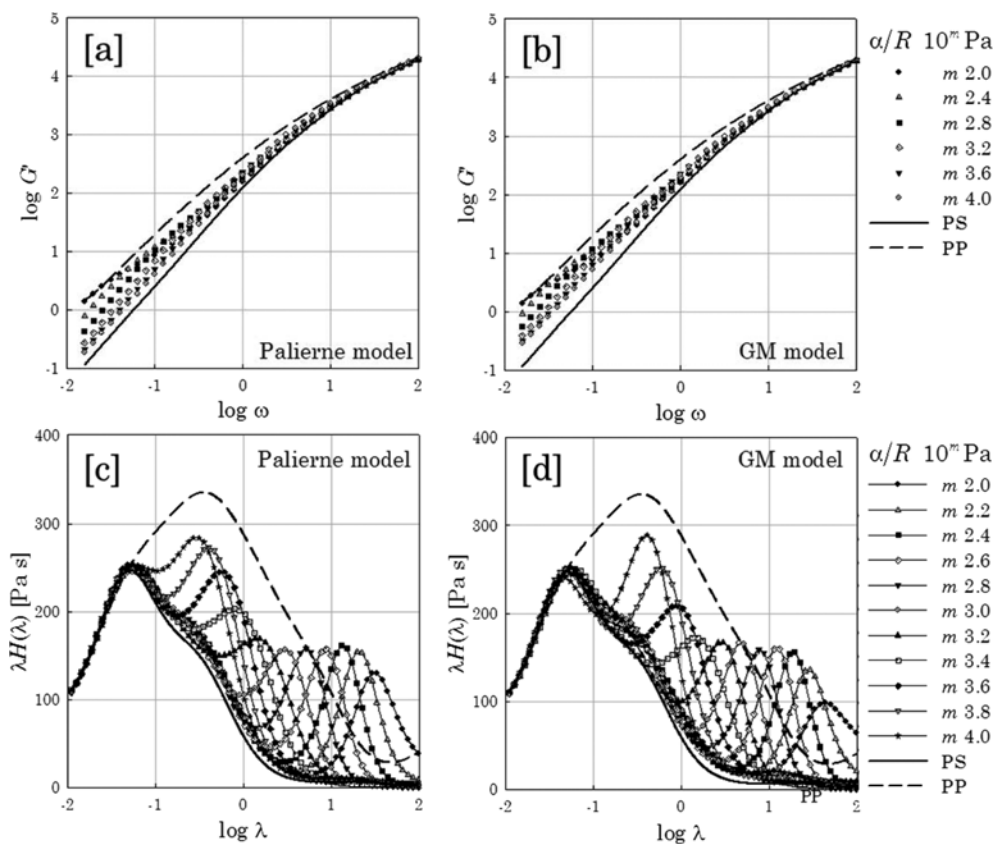


Fig. 4. Effect of the ratio α/R . Storage moduli generated from the Palierne model (a) and the GM model (b). Weighted relaxation time spectra are calculated from moduli using the Palierne model (c) and the GM model (d). Lines represent components and symbols or symbols with lines are blends with different α/R .

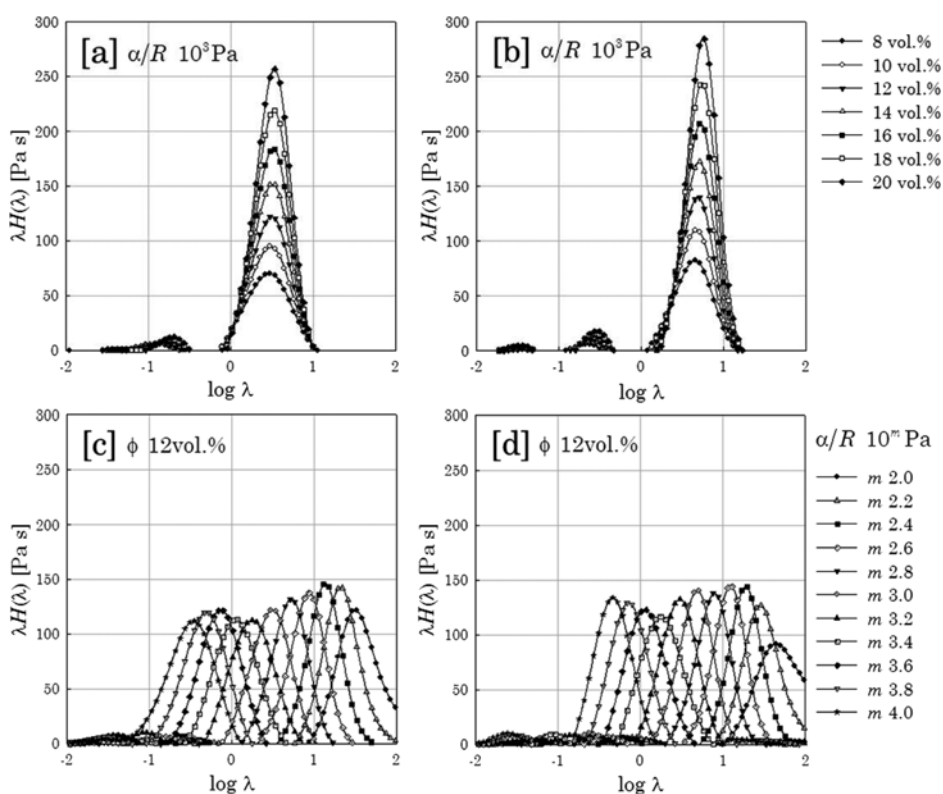


Fig. 5. Dependence of interfacial part of blends on the content of dispersed phase ((a) and (b)), the ratio α/R ((c) and (d)). (a) and (c) are results from the Palierne model and the results from the GM model are shown in (b) and (d).

of pure components from the weight relaxation spectrum of blends according to the picture of the GM model;

$$\lambda H_{\text{int}}(\lambda) = \lambda H_{\text{ble}}(\lambda) - \phi \lambda H_{\text{dis}}(\lambda) - (1 - \phi) \lambda H_{\text{mat}}(\lambda) \quad (22)$$

where $H_{\text{max}}(\lambda)$, $H_{\text{dis}}(\lambda)$, and $H_{\text{ble}}(\lambda)$ denote relaxation spectra of matrix, dispersed phase, and blend, respectively. $H_{\text{int}}(\lambda)$ is the remainder after extracting relaxation spectra caused by the components. From now on, we call it interfacial spectra. Fig. 5 shows the interfacial spectra defined by Eq. (22). Figs. 5a and 5b represent the effect of content of dispersed phase and Figs. 5c and 5d do the effect of

characteristic stress, α/R .

For quantitative comparison, we define λ_{max} as the relaxation time at the maximum of height in Fig. 5 and P_{max} as the maximum value of height. That is, $P_{\text{max}} \equiv \lambda_{\text{max}} H_{\text{int}}(\lambda_{\text{max}})$. The GM model gives P_{max} and λ_{max} as follows:

$$P_{\text{max}} = 2\eta_{\text{mat}}^{\circ} X_1(k, \phi), \quad (23)$$

$$\lambda_{\text{max}} = \frac{R}{\alpha} \eta_{\text{mat}}^{\circ} X_2(k, \phi) \quad (24)$$

where

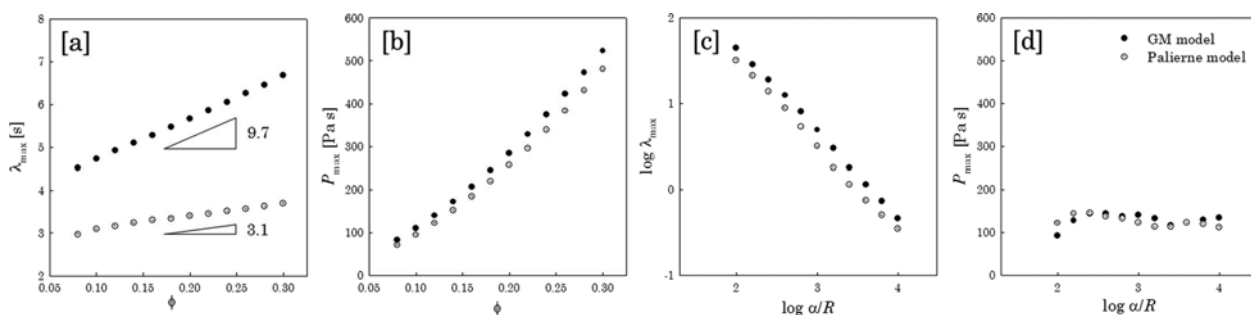


Fig. 6. Dependence of characteristics of the interfacial part on the content of dispersed phase ((a) and (b)) and the ratio α/R ((c) and (d)). (a) and (c) are changes of the position and those of the height are shown in (b) and (d). Filled circle is a result of interfacial part in weighted relaxation time spectra obtained from the GM model and open circle is a result using weighted spectra obtained from the Palierne model.

$$X_1 = \left[1 + \frac{5k+2}{2(2k+1)}\varphi + \frac{5(5k+2)^2}{8(k+1)^2}\varphi^2 \right] \cdot \frac{(19k+16)\varphi}{4(k+1)(2k+3)+5(19k+16)\varphi}, \quad (25)$$

$$X_2 = \frac{(19k+16)(2k+3)}{40(k+1)} \left[1 + \frac{5(19k+16)}{4(k+1)(2k+3)}\varphi \right]. \quad (26)$$

Eqs. (23) and (24) imply that when α/R is fixed, height and position of interfacial peak depend on only volume fraction of dispersed phase. Results in Figs. 5a and 5b agree with Eq. (23). When volume fraction of dispersed phase is fixed, peak height is independent of α/R while peak position depends on α/R linearly. Figs. 5c and 5d also show results consistent with Eq. (24), too. The GM model assumes the interfacial spectrum as the Dirac delta

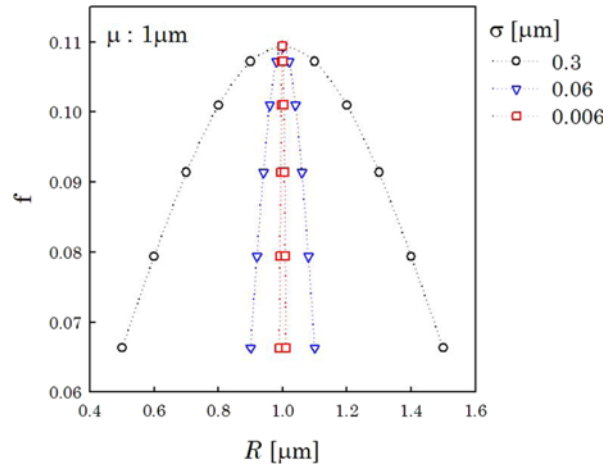


Fig. 7. (Color online) Gaussian distributions with the same mean but different standard deviation. The letters, μ and σ denote mean and standard deviation of radius of dispersions.

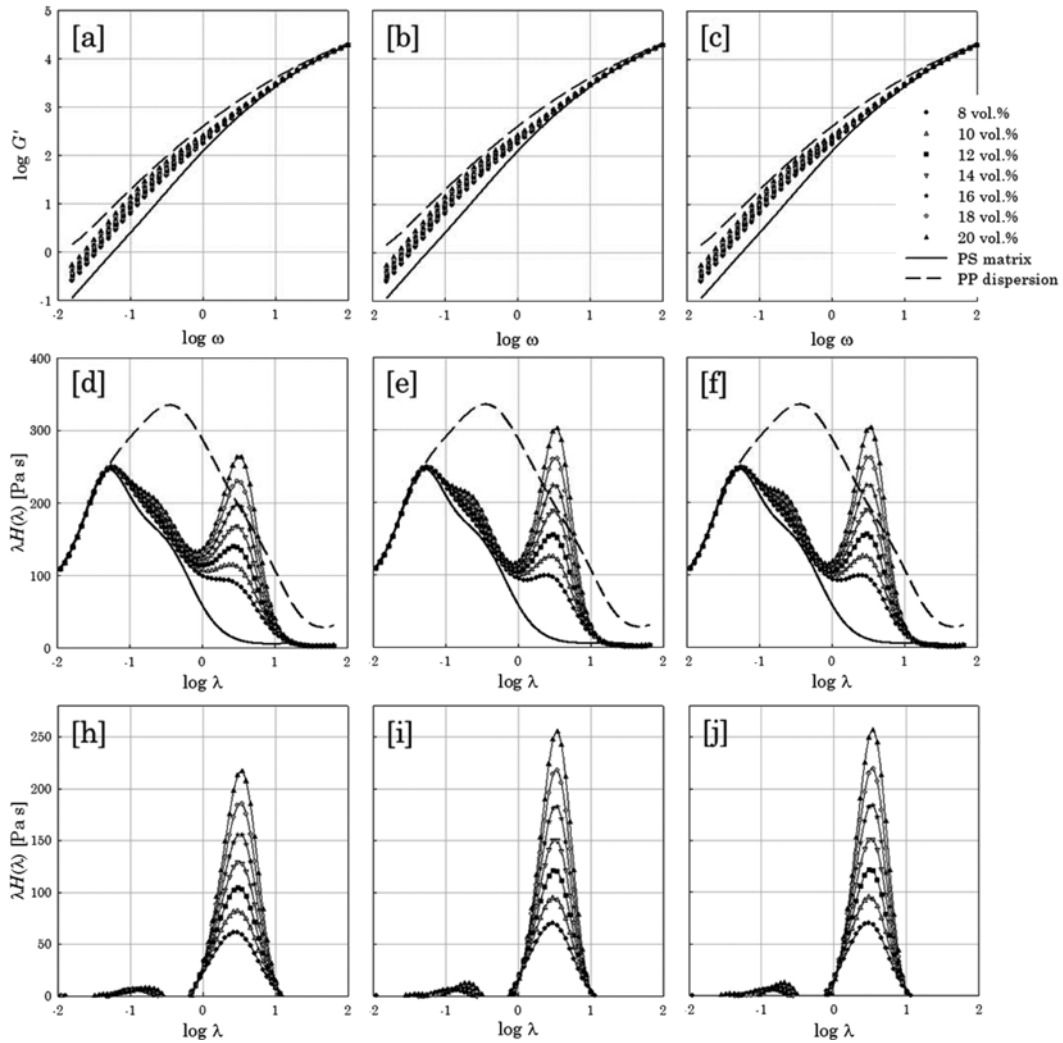


Fig. 8. Storage moduli, weighted relaxation time spectra, and interfacial parts of blends with different standard deviations of radius of dispersed phase, 0.3 μm ((a), (d) and (h)), 0.06 μm ((b), (e), and (i)) and 0.006 μm ((c), (f), and (j)). Lines represent dynamic moduli of components and symbols are those of blends with different contents of dispersed phase.

function while the spectra of Fig. 5 are continuous ones, which leads to slight variation of peak height in Figs. 5c and 5d. It is noteworthy that no algorithm cannot recover the Dirac delta from the simulated data even if modulus is generated from the spectrum of the Dirac delta function. Although spectrum of the Dirac delta function is not realistic, the GM model is helpful in understanding the relation between features of interfacial peak and structural parameters such as α/R and ϕ .

Fig. 6 clarifies the tendencies of height and position of peak in Fig. 5. The two models show very similar behaviors. However, a little difference is observed in peak position predicted by the two models at fixed α/R with varying volume fraction of dispersed phase. Although peak positions using the two models vary linearly with volume fraction, the slopes of the models are significantly different.

4.4. Effect of size distribution of dispersions

The Palierne model includes terms related with the effect of size distribution of dispersed phases. However, it is questionable whether such an effect can be detectable from linear viscoelastic data. Hence, we generated blend moduli whose dispersed phases follow the Gaussian size distributions shown in Fig. 7. The three distributions have the same mean of radius, 1mm while the standard deviations are different as indicated in Fig. 7.

The simulated storage moduli are shown in Fig. 8. No significant differences are observed in storage modulus and weighted spectrum, either. Hence, it can be said that no one can extract the information of the size distribution from linear viscoelastic data by use of the Palierne model.

5. Conclusions

It is well-known that blends present the relaxation of the interface through an additional peak in weighted relaxation time spectrum. This can be pictured out by the GM model. We have investigated the Palierne model quantitatively by the picture of the GM model which is simpler in equation but weaker in theoretical basis than the Palierne model.

In order to analyze the linear viscoelasticity of polymer blends, one may choose the Palierne model because of the rigorous theoretical foundation. However, it is difficult to understand how the interface contributes to the property of

blends at once due to the complexity of the model. In this study, we have shown that the Palierne model agrees with the result of Gramespacher and Meissner which is more intuitive. It implies that the Gramespacher-Meissner model is enough to substitute the Palierne model. Although the size distribution of dispersed phase is considered in the Palierne model, we found that the effect of the size distribution could be extracted from linear viscoelastic data.

Acknowledgements

This research was supported by Basic Science Research Program through the National Research Foundation of Korea (NRF) funded by the Ministry of Education, Science and Technology (NRF-2013R1A1A2055232).

References

- Baumgaertel, M. and H.H. Winter, 1992, Interrelation between continuous and discrete relaxation time spectra, *J. Non-Newton. Fluid Mech.* **44**, 15-36.
- Cho, K.S. and G.W. Park, 2013, Fixed-point iteration for relaxation spectrum from dynamic mechanical data, *J. Rheol.* **57**, 647-678.
- Choi, S.J. and W.R. Schowalter, 1975, Rheological properties of nondilute suspensions of deformable particles, *Phys. Fluids* **18**, 420-427.
- Doi, M. and T. Ohta, 1991, Dynamics and rheology of complex interfaces. I, *J. Chem. Phys.* **95**, 1242-1248.
- Graebbling, D., R. Muller, and J.F. Palierne, 1993, Linear viscoelastic behavior of some incompatible polymer blends in the melt. Interpretation of data with a model of emulsion of viscoelastic liquids, *Macromolecules* **26**, 320-329.
- Gramespacher, H. and J. Meissner, 1992, Interfacial tension between polymer melts measured by shear oscillations of their blends, *J. Rheol.* **36**, 1127-1141.
- Honerkamp, J., 1989, Ill-posed problems in rheology, *Rheol. Acta* **28**, 363-371.
- Honerkamp, J. and J. Weese, 1989, Determination of the relaxation spectrum by a regularization method, *Macromolecules* **22**, 4372-4377.
- Lee, H.M. and O.O. Park, 1994, Rheology and dynamics of immiscible polymer blends, *J. Rheol.* **38**, 1405-1425.
- Palierne, J.F., 1990, Linear rheology of viscoelastic emulsions with interfacial tension, *Rheol. Acta* **29**, 204-214.
- Shonaike, G.O. and G.P. Simon, 1999, *Polymer Blends and Alloys*, Marcel Dekker, New York.